SCIENCE CHINA
Technological Sciences

May 2012 Vol.55 No.5: 1189–1197
doi: 10.1007/s11431-012-4800-2

# The first time observations of low-latitude ionospheric irregularities by VHF radar in Hainan

NING BaiQi[1, 2*], HU LianHuan[1, 2, 3], LI GuoZhu[1, 2], LIU LiBo[1, 2] & WAN WeiXing[1, 2]

[1] *Institute of Geology and Geophysics, Chinese Academy of Sciences, Beijing 100029, China;*
[2] *Beijing National Observatory of Space Environment, Beijing 102213, China;*
[3] *Graduate University of Chinese Academy of Sciences, Beijing 100081, China*

Received December 12, 2011; February 10, 2012; published online March 26, 2012

Sanya VHF radar (18.4°N, 109.6°E, dip latitude 12.8°N) at Hainan Island is the first coherent backscatter radar for sounding low-latitude ionospheric irregularities in the mainland of China. In this paper, we present the first results of low-latitude ionospheric E and F region irregularities using the radar data during the period from February 2009 to March 2010. The Doppler velocity of radar echoes from E region field aligned irregularities (FAIs) was about several tens of meters per second, while the Doppler spectral width was appreciably larger than the velocity, and could reach one hundred meters per second, indicating that the observed E region FAIs belonged to type 2 irregularities. The observations of range time intensity (RTI) maps of FAIs showed that E region irregularities most often occurred at night within the altitude range 85–115 km, and were rarely observed at afternoon hours. The percentage occurrence of E region FAIs maximized during spring months (Feb.–May) with a peak value over 80%. The heights at which the strongest echo related FAIs occurred were mainly around 100 km, lower than h'Es and the difference is mostly 10–20 km. December solstice seemed to be the minimum period of occurrence when the FAI echoes were commonly detected at a narrow altitude range 90–100 km. Moreover, simultaneous radar and GPS observations during spread F events in the pre-midnight hours of solar minimum revealed that significant GPS L band scintillations coincided with the appearance of F region plasma plume structures, which extended up to 450 km in altitude.

**low-latitude ionosphere, ionospheric irregularities, VHF radar**

**Citation:** Ning B Q, Hu L H, Li G Z, et al. The first time observations of low-latitude ionospheric irregularities by VHF radar in Hainan. Sci China Tech Sci, 2012, 55: 1189–1197, doi: 10.1007/s11431-012-4800-2

## 1 Introduction

When a radio signal acts on the disturbed ionosphere, for example, the sporadic E (Es) or spread F structures, the received signal would show rapid fluctuations in amplitude and phase that is not consistent with the source strength or modulation. It is well known that ionospheric irregularity has the potential to affect satellite communication in a number of ways, from degradation of accuracy such as the range errors, to the loss of signal tracking. Since ionospheric irregularity producing scintillation can cause considerable communication hazards for radio systems and is therefore of great practical interest, it is generally recognized that further research on the generation and evolution of different scale size ionospheric irregularities is required, especially using high power large aperture radar measurements to investigate the echo type and spectral characteristics of small scale irregularities in detail.

Over the past several decades, the E region field-aligned irregularities (FAIs) in the equatorial electrojet (EEJ) and auroral electrojet regions have been extensively studied.

*Corresponding author (email: nbq@mail.iggcas.ac.cn)

Significant progress has also made in understanding the mid-latitude E region FAIs. Quasi periodic (QP) echoes from the E region FAIs were first reported by Yamamoto et al. (1991) using the middle and upper atmosphere (MU) radar located at Japan. Intensive efforts to obtain detailed information associated with Es layer and QP structures were the Sporadic E Experiment over Kyushu (SEEK-I) in 1996 and SEEK-II in 2002 [1–5]. Some explanations for the QP echoes, for example, the passing atmospheric gravity wave (AGW) modulate Es layer and neutral wind shear driven Kelvin-Helmholtz (KH) instability have been proposed [1–6]. At mid-latitude, the E region FAI is basically a nighttime phenomenon. The observations made on the FAI using radar and Es parameters from ionosonde indicated a close association between them. Similar efforts have been made over Chung-Li to study the occurrence characteristics of equatorial anomaly region FAIs [7–9]. The observations on low-latitude FAIs have just begun recently, only made by the Gadanki MST radar (3.5°N, 79.2°E, dip latitude 6.5°N) located in the southern part of India, and by the Piura VHF radar (5.2°S, 80.6°W, dip latitude 6.9°N) located in northern Peru [10–14]. These radars have revealed that the echo type and spectral characteristic of low-latitude FAIs are very similar to mid-latitude, but obviously different from those at EEJ region. A study on the possible link of the FAIs with Es layer activity over low-latitude will help to understand the generation mechanism of these structures [15, 16].

In Jan. 2009, a VHF coherent backscatter radar for sounding the low-latitude E and F region irregularities was installed at Sanya (18.4°N, 109.6°E, dip latitude 12.8°N), in Hainan Island, China by the Institute of Geology and Geophysics, Chinese Academy of Sciences. In this paper, we will be focusing on the statistical occurrence characteristics of E region FAIs and Es layer during the period from February 2009 to March 2010, and the correlations of them. We also present, for the first time, the Doppler spectral characteristics of E region FAI echoes and the simultaneous observations of different scale F region irregularities from multi instruments at Hainan.

## 2 Instruments and experimental details

The Sanya VHF radar, while designed primarily for coherent scatter study of ionospheric irregularities, was also intended for specular meteor trail observations. Accordingly, the alternative antenna is composed of two arrays, one for meteor and another for ionosphere. The ionosphere array consists of 24 five-element Yagi antennas and is arranged as two parallel rows aligned east-west (12×2). For the observations of FAIs, the antenna beam is positioned at a zenith angle of about 23° to the north, which satisfies the field perpendicular condition for coherent scatter at heights of the E region. Details of the antenna array please see Figure 1 of Li et al. (2012) [17]. Another capability of the radar is to steer the beam with a step of 2.5° within azimuth angle of ±45°. This configuration can be used to measure the zonal drifts of irregularities. The detailed characteristics of the Sanya VHF radar for FAI observations are summarized in Table 1. Another antenna array for meteor consists of one crossed dipole antenna for transmission and five crossed dipole antennas for reception. Under the all-sky meteor radar mode, the mean winds can be determined from the radial velocities of specular meteor trails [18].

Basically, the Sanya VHF radar operates in a successive sequence of 1 min under coherent backscatter mode and 1 min under all-sky meteor mode for routine observations of FAIs and mean winds. The evidence of equatorial plasma bubble bifurcation inducing low altitude E region FAI disruption and valley region FAI generation during post-sunset hours, planetary wave modulating E region FAI echoes and the wind comparison between range spread trail echoes and specular meteor trail echoes have been investigated recently using these measurements [17, 19, 20]. During the observational periods to be discussed in this paper, we used signal-to-noise ratio (SNR) measured by different observational modes, which were operated depending on echo range and time sample. The detailed characteristics of the modes are summarized in Table 2.

In order to investigate the amplitude and phase scintillation occurrence of GPS L1 band in Chinese low latitude region, two modified GPS receivers were setup at Sanya. The receiver is a NovAtel Euro4 dual-frequency receiver version with OEM4 card and special firmware, which also yields the value of ionospheric TEC [21]. The E region parameters from ionosonde are also available at a time interval

**Table 1** Radar parameters under coherent backscatter mode

| | |
|---|---|
| Geographic location | 109.6°E, 18.4°N |
| Operation frequency | 47.5 MHz |
| Peak power | 24 kW |
| Antenna array | 12×2 five element Yagi antennas |
| Antenna array area | 53.6 m×6 m |
| Antenna gain | 22 dB |
| Beam direction | 23°N |
| Beam width | 10° in east-west, 24° in north-south |
| Sweep mode | 2.5°/step, ±45° in east-west |

**Table 2** Radar specifications used for the FAI observations

| Operation mode | |
|---|---|
| Mode 1 | Feb., 2009–May, 2009 |
| Range coverage | 70–313 km |
| Range resolution | 1.8 km |
| Mode 2 | Jun., 2009 –Oct., 2009 |
| Range coverage | 80–200 km (day), 80–800 km (night) |
| Range resolution | 0.9 km (day), 4.8 km (night) |
| Mode 3 | Nov., 2009–Jan., 2010 |
| Range coverage | 80–200 km |
| Range resolution | 0.9 km |

of 15 min. In the present analysis, SNR measurements from VHF radar, foEs and h'Es from ionosonde and GPS scintillations were utilized to investigate the occurrence characteristics of irregularities and the correlation between them.

## 3 Results and discussion

Figure 1 shows the range-time-intensity (RTI) plots of the radar backscatter from E and F region irregularities under three observational modes on Mar. 6, July 22 and Nov. 15, 2009, respectively. The horizontal white (black) bar represents the local daytime (nighttime). The top panel (a) is a typical example of mode 1 with range and time bins of 1.8 km and 3 min, respectively. For the case of mode 2 presented in the middle panel (b), the range and time bins are 0.9 km and 2 min for daytime, and 4.8 km and 2 min for nighttime, respectively. The bottom panel (c) represents mode 3 with range and time bins 0.9 km and 2 min, respectively. As indicated, the FAI echoes may occur at daytime as well as nighttime under all the three modes.

Figure 1(a) displays E region echoes occurring at higher altitude range up to 160 km in the presence of F region irregularities, probably associated with the manifestation of F-E region coupling. The equatorial F region irregularities may extend along the magnetic field lines to low-latitude E region [22]. Furthermore, it is noteworthy that the E region FAI echoes occurred more frequently at night with stronger SNR than daytime (Figure 1(c)). During the sunset period 0900–1100 UT, the echo region descended slowly from 105 km to 90 km. Such a descending ionized layer could be formed due to tides or gravity waves which have a downward phase speed yielding the slow vertical descent, or are carried downward by a descending wind shear.

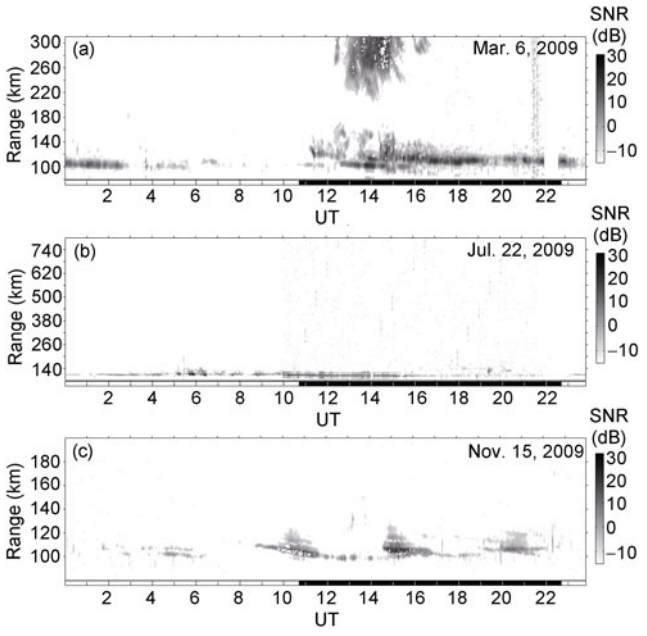


**Figure 1** The signal-to-noise ratio (SNR) values observed on (a) Mar. 06, 2009, (b) Jul. 22, 2009 and (c) Nov. 15, 2009. The horizontal black (white) bar respresents the local night (day) time.

### 3.1 Doppler spectra of E region FAIs

The spectral behavior of the radar returns from ionospheric irregularities, especially the Doppler velocity and Doppler spectral width are very important for investigating the dynamics of irregularities. The complex raw returns of Sanya VHF radar were recorded in the data storage unit and the 256-point fast Fourier transform (FFT) algorithm was employed to calculate the radar spectrum for each range gate and receiving channel. After employing coherent integration, we would get the normalized spectrum within 1 min interval. The moment method was used to calculate the zero moment ($m_0$), first moment ($m_1$) and second moment ($m_2$), then we obtained the corresponding mean Doppler velocity ($V_d$) and spectral width ($W_d$) of each spectrum, namely,

$$V_d = m_1/m_0, \tag{1}$$

$$W_d = (m_2/ m_0 - (m_1/m_0)^2)^{1/2}. \tag{2}$$

Figure 2(a) shows the height distribution of the Doppler spectra for the radar returns at 0624 UT on Jul. 22, 2009. Vertical bold and thin lines represent the mean Doppler velocity and spectral width of spectrum, respectively. Note that the Doppler velocities show a magnitude of several tens of meters per second (negative means toward the radar, i.e., downward/southward). As shown in the plot, the Doppler spectral width was appreciably larger than the velocity, and could reach one hundred meters per second, implying that the observed E region FAIs were due to gradient drift instabilities, i.e., type 2 irregularities [23]. However, the linear theory of the ionization gradient drift instability could not account for the Sanya VHF radar backscatter observations, which requires irregularity wavelengths of 3 m. It has been shown that the unstable waves do not steepen in the direction of propagation and attain large amplitudes, then become unstable to perturbations propagating in some other directions. The large-scale irregularities thus produce horizontal gradients much larger than the original vertical gradients and vertical drifts. These in turn lead to the generation of vertically propagating type 2 irregularities with wavelengths of several meters [24].

Figure 2(b) presents the variations of Doppler velocity versus range bin observed on Jul. 22, 2009 0300–1000 UT. It is clear from the figure that the scatter echoes continuously existed around 108 km range bins during 0430–1000 UT. However, for range bins above 110 km or below 107 km, multiple periodic echoes were observed. The Doppler velocity was apparently larger than those around 108 km. For FAI echoes, the Doppler velocities were interpreted as the line-of-sight projection of the E×B electron drift speeds, and Doppler shifted by the neutral winds. Since Sanya VHF the

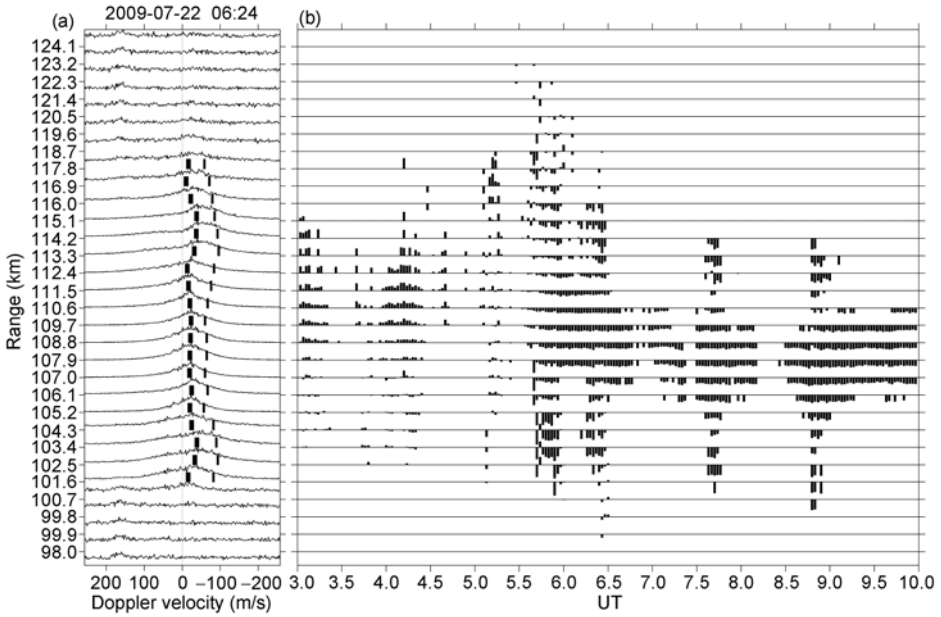


**Figure 2** (a) Doppler spectra for the radar returns at 0624 UT on Jul. 22, 2009. The vertical bold and thin lines represent the Doppler velocity and spectral width, respectively; (b) variation of FAI Doppler velocity measured during the period 0300–1000 UT.

radar points to 23° ($\theta$) to the north and becomes perpendicular to the E region magnetic field, the observed Doppler velocity can be represented as $\boldsymbol{V}_d \sim [\boldsymbol{E}\times\boldsymbol{B}/(1+\psi) + \psi\boldsymbol{V}\sin\theta/(1+\psi)]$, where $\psi$ is the anisotropy factor defined by the ion-neutral collision frequencies and cyclotron frequencies. In the present case, the height region (<100 km in altitude) was collision dominated, $\psi \geqslant 1$, the Doppler velocities at these heights might be attributed to the meridional winds $\boldsymbol{V}$. Under this consideration, we probably can derive the meridional wind speed from the Doppler velocity measurements of lower E region FAIs.

### 3.2 Statistical occurrence characteristics of E region FAIs

To show the statistical occurrence characteristics of the E region FAIs over Sanya, we present the percentage occurrence of E region echoes as a function of local time, height and month. A threshold value of SNR more than −5 dB was used in the statistical results. It is clear from Figure 3 that most of the daytime E region FAI echoes appeared at the heights from 85 to 105 km, and there was no echo detected above 115 km. The echo occurrence rates during the noon and afternoon periods (0500–1000 UT) were less than those at other times. Moreover, during the December solstice (Nov.–Jan.), the E region FAI echoes were confined to a lower altitude range 90–100 km and mainly occurred at nighttime, almost no daytime E region echo was observed. When we note the percentage occurrence of the nighttime E region echoes during other months, it can be seen from the figure that there were two regions with significant occurrence, one was below the 100 km that is similar to the daytime echoes, and the other was between 100 and 120 km. For nighttime echoes observed at higher altitude above 100 km, the maximum occurrence time interval was between 1400 and 2200 UT during Mar.–May. As it can be seen from the left bottom panel of Figure 3, the layered structures appeared during the post-sunset hours.

When comparing the morphological features of E region FAI echoes observed by the three low-latitude radars, Gadanki, Piura and Sanya, we found that the general features were similar for the FAI echoes observed at Gadanki and Sanya, but very different from Piura during noon hours. For all three radars, the daytime FAI echoes were observed in the lower altitude regions, and spread to higher altitudes during nighttime as compared to daytime observations. The higher altitude echoes appeared only in the nighttime with maximum occurrence from midnight to morning hours. The echoing region showed layered structures, with thick patchy structures above or in the both sides of the middle layer near post-sunset. However, during noon hours, the echoes disappeared at Piura [25–27] whereas they occurred frequently at Sanya and Gadanki. Table 3 lists a comparison of radar parameters. It is clear from the table that the peak power of Sanya VHF radar was close to Piura radar, but Sanya VHF radar frequently detected noontime echoes, indicating that the transmitted peak power was not a critical parameter for the absence of noontime echoes. Such a difference could be attributed to the varying wind fields at geographically different locations [26].

Echo occurrence revealed from Sanya VHF radar observations showed that the diurnal characteristics of E region echoes were close to those observed at mid-latitude which occurred most often in the forenoon and nighttime hours,

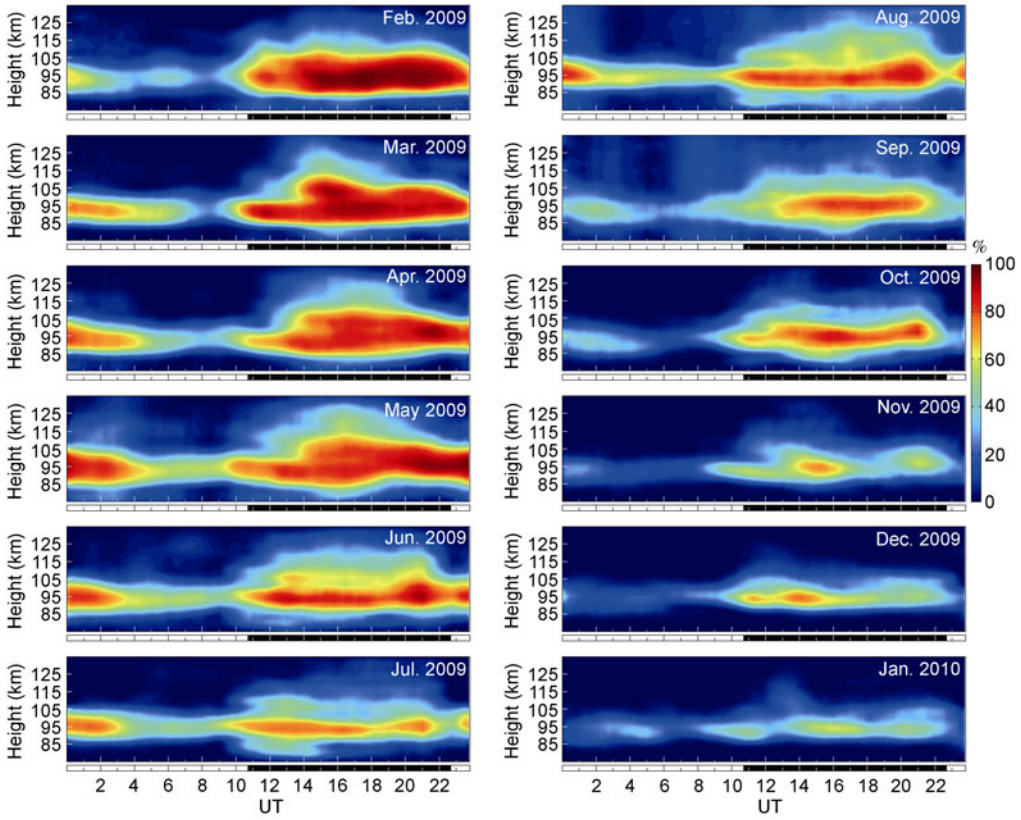


**Figure 3** Height-time variation of percentage occurrence of FAIs (with a threshold value of SNR>−5 dB) during Feb. 2009–Jan. 2010.

**Table 3** A comparison of low-latitude VHF radar parameters

| | Sanya | Gadanki | Piura |
|---|---|---|---|
| Peak power | 24 kW | 2.5 MW | 20 kW |
| Antenna array area | 320 m² | 12000 m² | 10000 m² |
| Duty cycle | 0.38%–1.6% | 0.4% | 0.66% |

and distinctly different from those of EEJ which were most intense around the noon hours. The spectral characteristics of Sanya VHF radar returns showed the E region FAIs belonged to type 2 irregularities, associated with the gradient drift instability [28]. At mid-latitude, the seasonal variations of E region FAI echoes showed a summer maximum. However, the Sanya VHF radar observations showed that the echo occurred with a maximum during February-May, probably indicating a combined influence of background density, Es layer, electric field and wind field on the seasonal variations of FAI echoes over Sanya.

### 3.3 Relationship between the E region FAI and Es layer

At EEJ region the vertical polarization Hall electric field driven by the primary E-layer dynamo electric field, is responsible for the gradient E×B drift (type 2) irregularities that manifests as q-type Es in the ionograms. Using the coherent backscatter from FAIs in the mid-latitude E region, Haldoupis and Schlegel [29] investigated the seasonal and diurnal variations of Es and FAI occurrence and found a close relationship between them. For the low-latitude region outside the EEJ, for example, Sanya, the electric fields are small as compared to the EEJ, and Es activities are relatively less compared to mid-latitude. In the following we present a case of simultaneously observed FAI and Es layer at Sanya, and the statistical association between the occurrence of radar FAI echoes and Es.

Figure 4 shows the signal strength of the FAI and Es parameters foEs and h'Es observed on 12 Mar. 2009. As shown in the top panel, echoes were found to be strong near 0200 UT, and afterwards became weak. Descending layered structures appeared until 1600 UT. This feature is common over Sanya as presented in Figure 3. The structures seen from the middle layer echoes were quasi-periodic (QP), which might be created by the K-H instability due to a sheared zonal neutral wind profile in the E region [30]. And also Tsunoda et al. proposed that at mid-latitude the Es layer at a zonal wind shear node was unstable at night to produce QP structures [31]. The wind shear velocity and the alignment of Es layer could influence the slop of QP structures. The period, slope, radial velocity and spectral width of the observed QP echoes will be discussed in another paper. As shown in the middle and bottom panels, the Es layer was observed during the period 0000–0300 UT, 0800–1000 UT and 1400–2000 UT. The maximum foEs was found to be

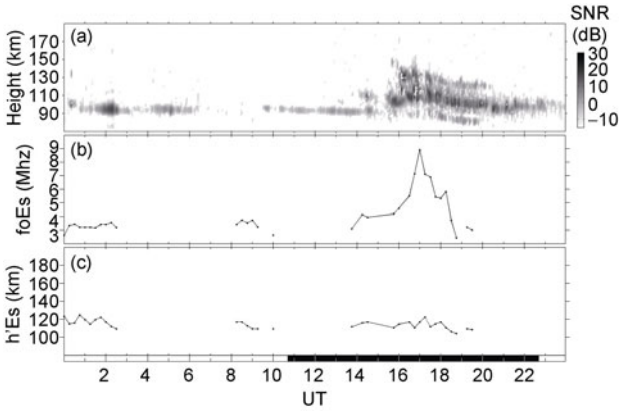


**Figure 4** (a) Height-time-intensity (HTI) map of the FAI; (b) and (c) variations of the E region parameters foEs and h'Es observed on March 12, 2009.

9 MHz occurring around 1700 UT, when the echo region showed layered structures. The h'Es remained a constant value about 120 km. In general the height of FAI was found to be 20 km lower than h'Es, except for a period at around 1600–2000 UT when the layered FAI echoes covered a wider altitude region.

In Figure 5, we present the statistical occurrence probability of FAIs and Es layer. It is clearly evident from the figure that at night the occurrence of FAIs was apparently higher than Es layer, especially during Feb.–Apr., the occurrence difference was about 60%. While during daytime, the occurrence of FAIs was found to be comparable to Es layer. At low-latitude (outside EEJ), the electric fields were small as compared to the EEJ, and Es activities were relatively less compared to the mid-latitude. Thus, the low-latitude E region FAI occurrences were probably related to Es layer activity (providing density gradient required for gradient drift instability) and EEJ strength [27, 32].

Figure 6 presents the statistics of h'Es and the height of strongest echo related to FAIs as a function of time and month. The heights at which the daytime FAIs occurring were lower than h'Es and this difference was mostly 10–20 km. During nighttime, the difference was about 10 km and showed a highly scattered pattern, especially during Nov.–Dec. It may be mentioned that h'Es was the virtual height of Es layer and the true height would be a few kilometers less than h'Es. For the mid-latitude station of Shigaraki, Ogawa et al. found that the heights of the radar echoes in the morning hours were at 10–20 km below the h'Es. During daytime, when the polarization electric is upward, the positive gradient of electron density existing at the bottomside of the peak Es layer is expected to be unstable through gradient drift instability. Accordingly, the FAI was expected to occur at height where gradient is maximum and that is expected to be below the peak of the Es layer [33]. During nighttime, the E region electron density profile often shows jaggedness [34]. Hence, the nighttime FAI could be expected at several height regions where the instability criteria are satisfied.

### 3.4 Radar observations of F region plasma plume structures

The observations of F region irregularities presented here were made at solar minimum years, 2009–2010. During the

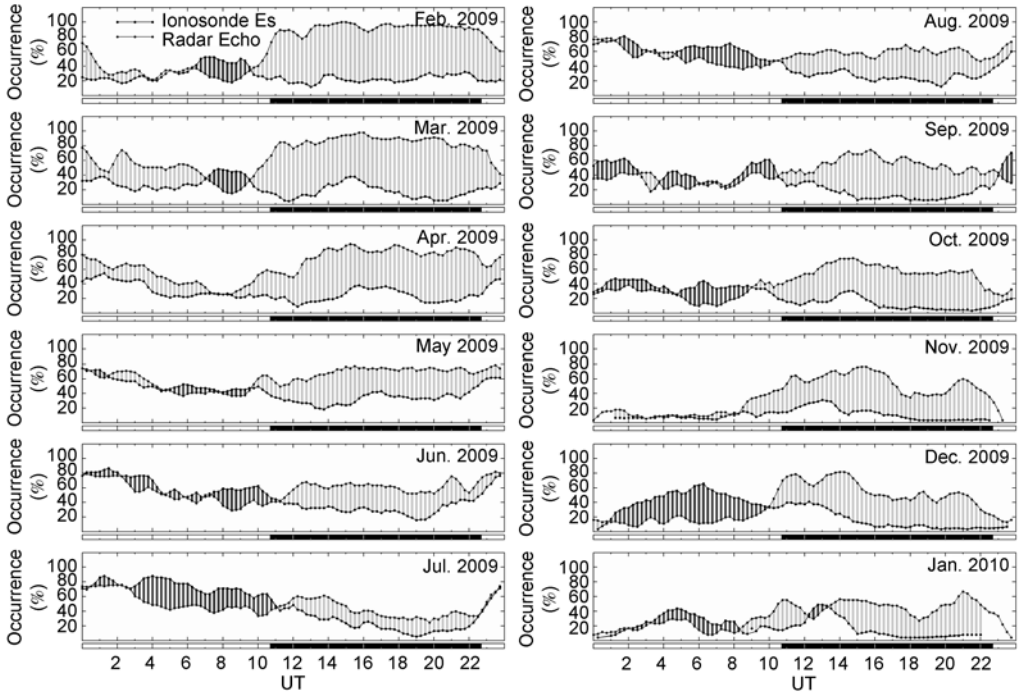


**Figure 5** Diurnal variation of E region FAI occurrence (with a threshold value of SNR > –5 dB) and Es layer during Feb. 2009–Jan. 2010.

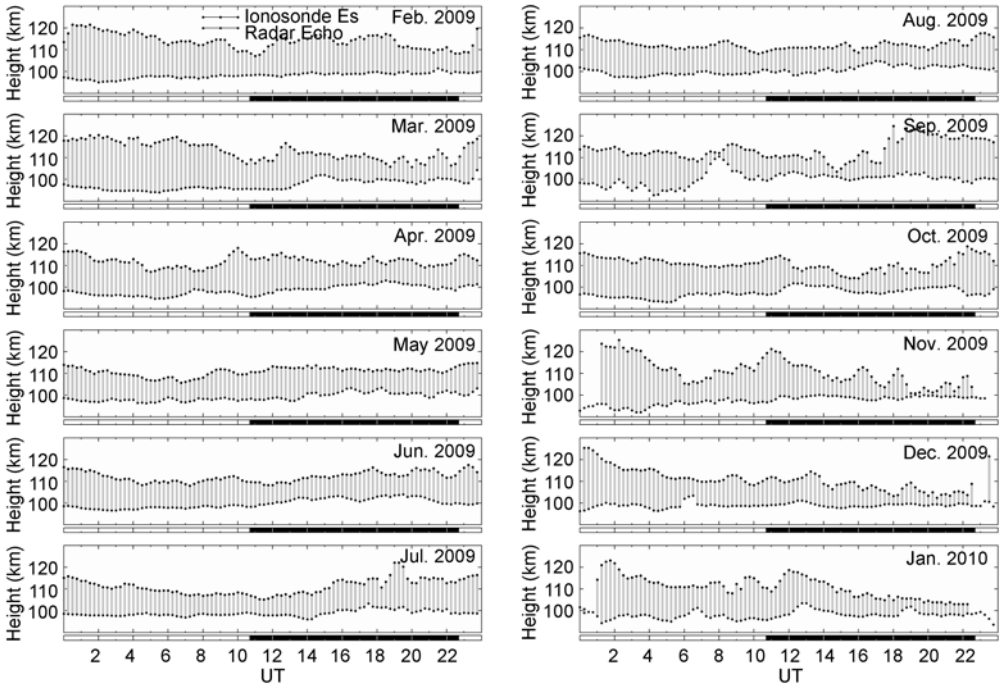


**Figure 6** A statistical comparison of h'Es and the height of most intense FAI echoes observed during Feb. 2009–Jan. 2010.

pre-midnight period of 2009, F region irregularities were only observed on nine nights by Sanya VHF radar (we should note that at times the sampling range of Sanya VHF radar was confined below 200 km; see Table 2). By utilizing the simultaneous measurements from ionosonde and GPS receivers, spread F structures and GPS ionospheric scintillations were observed concurrently. Figure 7 shows an example of a RTI map obtained by the VHF radar and simultaneous GPS scintillation on 2 Mar. 2010. Strong range type spread F structures can be seen from simultaneous ionograms which are not shown here. The RTI map shows low altitude irregularities developing from 1200 UT around 190 km, and then rapidly exploding into high altitude plume structures. The plasma plumes are interpreted as a manifestation of large plasma depletions known as plasma bubbles that originate in the bottomside F region and may extend over several hundred kilometers in altitude [35, 36]. Near the beginning of plasma plumes, the peak height of F layer hmF2 increased apparently. The range type spread F firstly occurred in the bottomside of F region and then evolved into a strong spread layer with thickness over 200 km. It is clear from the figure that the maximum intensity of GPS scintillation coincides well with the strongest F region echoes.

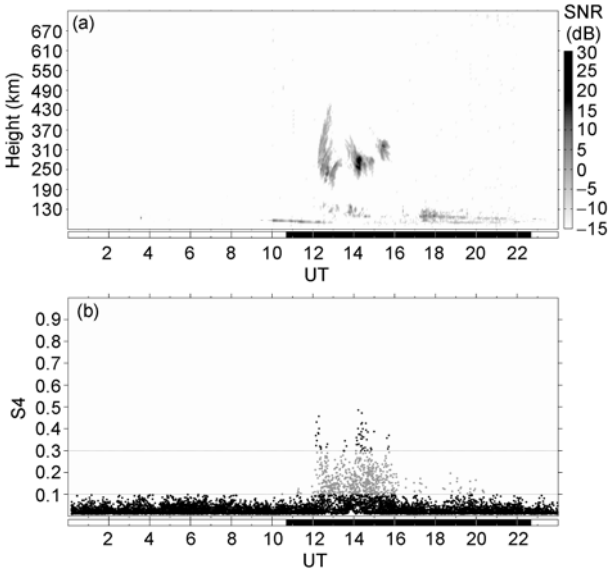


**Figure 7** (a) Plasma plume structures observed by Sanya VHF radar on Mar. 2, 2010; (b) scintillation index (S4) computed for the high elevation GPS satellite signals.

Since the Sanya VHF radar operates at a frequency of 47.5 MHz, the observed plasma plume structures correspond to a small scale of about 3 m. According to scintillation theory, L1 GPS signals are sensitive to about 400 m scale size irregularities situated at the 350 km altitude. The range type spread F structures on ionograms are due to the reflection of radio waves from kilometric scale size irregularities with structures as small as 3 m below or near the base of the F-region. The concurrent observations from VHF radar, ionosonde and GPS scintillation receiver have indicated that over Sanya, different scale size irregularities co-exist during pre-midnight hours, similar to the equatorial observational results [20, 35].

## 4 Conclusion

Based on more than 1 year of continuous observations of

irregularities by Sanya VHF coherent scatter radar, together with the simultaneous measurements from ionosonde and GPS scintillation receiver, we presented the morphological characteristics of the E region FAI echoes and Es layer, and the features of F region irregularities. The main findings are as follows.

1) The Doppler velocity of radar echoes from E region FAIs over Hainan is about several tens of meters per second, while the Doppler spectral width is appreciably larger than the velocity, and can reach one hundred meters per second, indicating that the observed E region FAIs belong to type 2 irregularities.

2) Seasonal variations of E region FAI echoes show that they occur over the entire year with maximum in spring equinoctial months (Feb.–May), moderate in summer and autumn months (Jun.–Oct.). In other months (Nov.–Jan.), echo occurrence shows low values or total disappearance during afternoon hours, and is confined at a narrow altitude range.

3) E region FAI echoes may occur in daytime as well as in nighttime. But the occurrence rates, the height extent, and the SNR strength of nighttime echoes are apparently larger than those of daytime. Afternoon seems to be the minimum period of occurrence.

4) Diurnal variations of E region FAIs and Es parameters (foEs and h'Es) are found to be related. The statistical analysis shows that the occurrence of daytime Es layer is correlated well with FAI echo occurrence. The heights at which the strongest echo related FAIs occur are mainly around 100 km, lower than h'Es and the difference is mostly 10–20 km. During nighttime, the echoes occur more frequently than the Es layers.

5) Case study of simultaneous observations of pre-midnight F region plasma plumes, spread F structures and GPS scintillations shows a close relationship between them, which is in agreement with the evolution characteristics of equatorial F region irregularities.

Although numerous studies on the characteristics of E and F region irregularities using VHF coherent scatter radar have been presented, none has been performed in the main land of China. This paper, for the first time, presents the Doppler spectral characteristics and the occurrence rates of radar FAI echoes by Sanya VHF coherent scatter radar in Hainan. By utilizing the radar raw power data, together with the multi instruments located at or around Sanya, we wish to examine the source energy for the generation of E region FAIs to understand the processes in detail. It is quite possible that the planetary wave modulations and the coupling of E and F region could play an important role in the day-to-day variability of E region FAI occurrence. Moreover, F region irregularity measurements from Sanya VHF radar will improve our understanding of the generation and dynamics of low-latitude plasma plume structures in Chinese longitude.

*This work was supported by the National Natural Science Foundation of China (Grant Nos. 41074113, 40904038, 40774091, 41174136) and Chinese Academy of Sciences (Grant No. KZCX2-YW-Y10). The authors are grateful to Wu Baoyuan and Sanya station technical staff for their dedicated efforts for making the observations reported here.*

1 Yamamoto M, Fukao S, Woodman R F, et al. Midlatitude E-region field-aligned irregularities observed with the MU radar. J Geophys Res, 1991, 96: 15943–15949
2 Kelley M C, Riggin D, Pfaff R F, et al. Large amplitude quasi-periodic fluctuations associated with a mid-latitude sporadic E layer. J Atmos Terr Phys, 1995, 57: 1165–1178
3 Hysell D L, Burcham J D. HF radar observations of quasiperiodic E layer echoes over North America. J Geophys Res, 1999, 104: 4361–4371
4 Tsunoda R T, Burnocore J J, Saito A, et al. First observations of quasi periodic radar echoes from Stanford, California. Geophys Res Lett, 1999, 26: 995–998
5 Haldoupis C, Hussey G C, Bourdillon A, et al. Azimuth-time-intensity striations of quasi periodic radar echoes from the midlatitude E-region ionosphere. Geophys Res Lett, 2001, 28: 1933–1936
6 Pan C J, Larsen M F. Observations of QP radar echo structure consistent with neutral wind shear control of the initiation mechanism. Geophys Res Lett, 2000, 27: 867–870
7 Pan C J, Liu C H, Rottger J, et al. A three-dimensional study of E-region irregularity patches in the equatorial anomaly region using the Chung-Li VHF radar. Geophys Res Lett, 1994, 21: 1763–1766
8 Chu Y H, Wang C Y. Interferometric observations of 3-dimensional spatial structure of sporadic E irregularities using Chung-Li VHF radar. Radio Sci, 1997, 32: 817–832
9 Pan C J, Tsunoda R T. Quasi-periodic echoes observed with the Chung-Li VHF radar during the SEEK campaign. Geophys Res Lett, 1998, 25: 1809–1812
10 Krishnamurthy B V, Ravindran S, Viswanathan K S, et al. Small-Scale (~3m) E-region irregularities at and off the magnetic equator. J Geophys Res, 1998, 103: 20761–20772
11 Patra A K, Rao P B. High resolution radar measurements of turbulent structure in the low-latitude E-region. J Geophys Res, 1999, 104: 24667–24673
12 Patra A K, Sripathi S, Sivakumar V, et al. Evidence of kilometer scale waves in the lower E-region using high resolution VHF radar over Gadanki. Geophys Res Lett, 2002, 29(10): 1499
13 Patra A K, Rao P B, Anandan V K, et al. Evidence of intermediate layer characteristics in the Gadanki radar observations of the upper E-region field-aligned irregularities. Geophys Res Lett, 2002, 29(14): 1696
14 Woodman R F, Chau J L, Aquino F, et al. Low latitude field-aligned irregularities observed in the E region with the Piura VHF radar: first results. Radio Sci, 1999, 34: 983–990
15 Lee C C, Liu, J Y, Pan C J. The heights of Sporadic-E layer simultaneously observed by the VHF radar and ionosondes in Chung-Li. Geophys Res Lett, 2000, 27: 641–644
16 Phanikumar D V, Patra A K, Devasia C V, et al. Seasonal variation of low-latitude E-region plasma irregularities studied using Gadanki radar and ionosonde. Ann Geophys, 2008, 26: 1865–1876
17 Li G, Ning B, Hu L, et al. A comparison of lower thermospheric winds derived from range spread and specular meteor trail echoes. J Geophys Res, 2012, 117: A03310, doi:10.1029/2011JA016847
18 Hocking W K, Fuller B, Vandepeer B. Real-time determination of meteor-related parameters utilizing modern digital technology. J Atmos Sol-Terr Phys, 2001, 63: 155–169
19 Li, Z., Ning B. Planetary scale wave observations over low-latitude E region using simultaneous observations of VHF radar and ionosonde

over Sanya (18.34 degrees N, 109.62 degrees E). J Geophys Res, 2010, doi:10.1029/2010JA015816

20 Li G, Ning B, Patra A K, et al. Investigation of low-latitude E and valley region irregularities: Their relationship to equatorial plasma bubble bifurcation. J Geophys Res, 2011, 116: A11319, doi:10.1029/2011JA016895

21 Li G, Ning B, Hu L, et al. Longitudinal development of low−latitude ionospheric irregularities during the geomagnetic storms of July 2004. J Geophys Res, 2010, 115: A04304, doi:10.1029/2009JA014830

22 Patra A K. Some aspects of electrostatic coupling between E and F regions relevant to plasma irregularities: A review based on recent observations. J Atmos Sol-Terr Phys, 2008, 70: 2159–2171

23 Balsley B B. Some characteristics of non-two-stream irregularities in the equatorial electrojet. J Geophys Res, 1969, 74: 2333–2347

24 Sudan R N, Akinrimisi J, Farly D T. Generation of small-scale irregularities in the equatorial electrojet. J Geophys Res, 1973, 78: 240–248

25 Pan C J, Rao P B. Morphological study of the field-aligned E-layer irregularities observed by the Gadanki VHF radar. Ann Geophys, 2004, 22: 3799–3804

26 Patra A K, Sripathi S, Sivakumar V, et al. Statistical characteristics of VHF radar observations of low latitude E-region field-aligned irregularities over Gadanki. J Atmos Solar-Terr Phys, 2004, 66: 1615–1626

27 Chau J L, Woodman R F, Flores L A. Statistical characteristics of low latitude ionospheric field-aligned irregularities obtained with Piura VHF radar. Ann Geophys, 2002, 20: 1203–1212

28 Raghavarao R, Patra A K, Sripathi S. Equatorial E region irregularities: A review of recent observations. J Atmos Solar-Terr Phys, 2002, 64: 1435–1443

29 Haldoupis C, Schlegel K. Characteristics of mid-latitude coherent backscatter from the ionospheric E region obtained with Sporadic E Scatter experiment. J Geophys Res, 1996, 101: 13387–13398

30 Larsen M F. A shear instability seeding mechanism for quasiperiodic radar echoes. J Geophys Res, 2000, 105: 24931–24943

31 Tsunoda R T, Fukao S, Yamamoto M. On the origin of quasi-periodic radar backscatter from mid-latitude sporadic E. Radio Sci, 1994, 29: 349–362

32 Krishna B V, Ravindran S, Viswanathan K S, et al. Small scale (_3 m) E region irregularities at and off the magnetic equator. J Geophys Res, 1998, 103: 20761–20772

33 Patra A K, Sripathi S, Rao P B, et al. Simultaneous VHF radar backscatter and ionosonde observations of low-latitude E region. Ann Geophys, 2005, 23: 773–779

34 Prakash S, Subbaraya B H, Gupta S P. Rocket measurements ionisation irregularities in the equatorial ionosphere at Thumba and identifications of plasma irregularities. Indian J Radio Space Phys, 1972, 1: 72–80

35 Rodrigues F S, Paula E R, Abdu M A, et al. Equatorial spread F irregularity characteristics over Sao Luis, Brazil, using VHF radar and GPS scintillation techniques. Radio Sci, 2004, doi: 10.1029/2002RS-002826

36 Li G, Ning B, Zhao B, et al. Characterizing the 10 November 2004 storm-time middle-latitude plasma bubble event in Southeast Asia using multi-instrument observations. J Geophys Res, 2009, 114: A07304, doi:10.1029/2009JA014057